HYDROTHEMAL ALTERATION MAPPING USING FEATURE-ORIENTED PRINCIPAL COMPONENT SELECTION (FPCS) METHOD TO ASTER DATA: WIKKI AND MAWULGO THERMAL SPRINGS, YANKARI PARK, NIGERIA

Aliyu Ja'afar Abubakar , Mazlan Hashim*, and Amin Beiranvand Pour

Geoscience and Digital Earth Centre (INSTeG)
Research Institute for Sustainability and Environment (RISE)
Universiti Teknologi Malaysia (UTM)
81310 UTM Skudai, Johor Bahru, Malaysia
*Corresponding author: mazlanhashim @utm.my

Commission VI, WG VI/4

KEY WORDS: FPSC; ASTER; Hydrothermal alteration; Yankari Park; Nigeria

ABSTRACT:

Geothermal systems are essentially associated with hydrothermal alteration mineral assemblages such as iron oxide/hydroxide, clay, sulfate, carbonate and silicate groups. Blind and fossilized geothermal systems are not characterized by obvious surface manifestations like hot springs, geysers and fumaroles, therefore, they could not be easily identifiable using conventional techniques. In this investigation, the applicability of Advanced Spaceborne Thermal Emission and Reflection Radiometer (ASTER) were evaluated in discriminating hydrothermal alteration minerals associated with geothermal systems as a proxy in identifying subtle Geothermal systems at Yankari Park in northeastern Nigeria. The area is characterized by a number of thermal springs such as Wikki and Mawulgo. Feature-oriented Principal Component selection (FPCS) was applied to ASTER data based on spectral characteristics of hydrothermal alteration minerals for a systematic and selective extraction of the information of interest. Application of FPCS analysis to bands 5, 6 and 8 and bands 1, 2, 3 and 4 datasets of ASTER was used for mapping clay and iron oxide/hydroxide minerals in the zones of Wikki and Mawulgo thermal springs in Yankari Park area. Field survey using GPS and laboratory analysis, including X-ray Diffractometer (XRD) and Analytical Spectral Devices (ASD) were carried out to verify the image processing results. The results indicate that ASTER dataset reliably and complementarily be used for reconnaissance stage of targeting subtle alteration mineral assemblages associated with geothermal systems.

1. INTRODUCTION

Remote sensing satellite sensors have been used for detection of prospective geothermal sites by capability of mapping hydrothermal alteration mineral assemblages and thermal anomaly in the visible and near-infrared (VNIR), shortwave infrared (SWIR) and thermal infrared (TIR) portions of the electromagnetic spectrum (Littlefield and Calvin, 2015). Availability and significant improvement in spectral resolution of satellite remote sensors such as the Advanced Spaceborne Thermal Emission and Reflection Radiometer (ASTER) in the VNIR and SWIR bands increases the capability of mapping subtle alteration mineral features associated with concealed and fossilized geothermal systems (Pour and Hashim, 2014).

The VNIR subsystem of ASTER has three recording channels between 0.52 and 0.86 μm with a spatial resolution of up to 15 m. The SWIR subsystem of ASTER has six recording channels from 1.6 to 2.43 μm, at a spatial resolution of 30 m. ASTER swath width is 60km (each individual scene is cut to a 60x60 km2 area) which makes it useful for regional mapping (Abrams, 2000; Yamaguchi and Naito, 2003; Pour and Hashim, 2015).

Concealed and fossilized geothermal systems are not characterized by obvious surface manifestations like hot springs, geysers and fumaroles, therefore, they could not be easily identifiable using conventional techniques (Norton, 1984). Geothermal systems are essentially associated with hydrothermal alteration mineral assemblages such as iron oxide/hydroxide, clay, sulfate, carbonate and silicate groups, which are produced by surface alteration of primary minerals as a result of metasomatism or contact of the hot fluids derived from magmatic intrusions (Pournamdari et al, 2014a,b; Calvin and Pace, 2016). Accordingly, depending on the spatial and spectral resolution of the satellite remote sensor, hydrothermal alteration mineral groups associated with the geothermal system could be identified using spectral bands in the VNIR and SWIR regions.

The main objective of this investigation is to evaluate the applicability of ASTE VNIR and SWIR bands for identifying subtle hydrothermal alteration mineral features associated with concealed and fossilized geothermal systems in Yankari Park, northeastern Nigeria.

2. MATERIALS AND METHODS

2.1 Geology of the study area

The Yankari Park is located within Latitude 09° 75′ 00″ N, and Longitude 10° 50′ 00″ E in the south-central part of Bauchi State, northeastern Nigeria (Fig. 1). It covers an area of about 2244 km^2. Yankari National Park lies in the southern part of the Sudan Savannah. It is composed of savannah grassland with well-developed patches of woodland. It is also a region of rolling hills, mostly between 200 m and 400 m. The Yankari Park is situated in the Benue Trough, bordered to the west by the basement complex crystalline rocks of the Jos Plateau, to the northeast by the Biu Plateau and to the southeast by the Adamawa highlands (Ajakaiye et al., 1988). Kerri formation characterized by Cenozoic to Mesozoic sedimentary rocks is dominated lithological sequence in the study area. However, there are many extinct volcanic features in the Jos Plateau and the northeastern and western part of the Yankari Park.

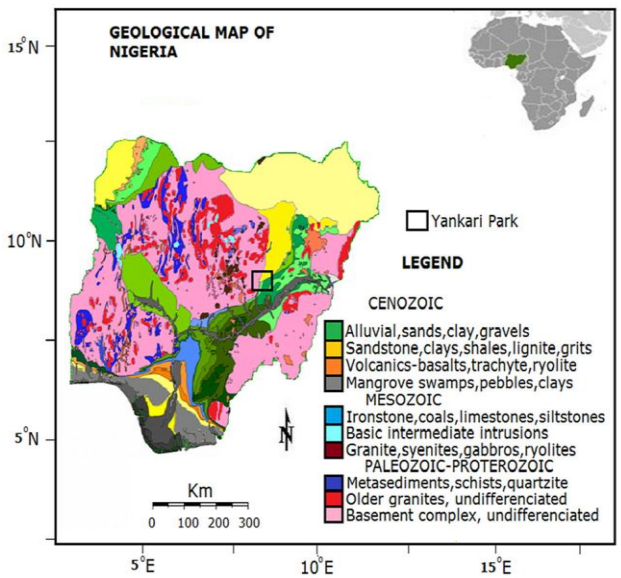

Figure 1. Geological Map of Nigeria showing the location of Yankari Park.

2.2 ASTER remote sensing data

Two cloud-free ASTER level 1T (Precision Terrain Corrected Registered At-Sensor Radiance) scene (AST_L1T_00301252006095330 and AST_L1T_00311142008095512 path/raw, 187/53) covering the Yankari Park were obtained from U.S. Geological EROS. The images have January 25th, 2006 and January 1st, 2003 acquisition dates, respectively. The ASTER Level 1 Precision Terrain Corrected Registered At-Sensor Radiance (AST_L1T) data contains calibrated at-sensor radiance, which corresponds with the ASTER Level 1B (AST_L1B), that has been geometrically corrected, and rotated to a north up UTM projection. The images were pre-georeferenced to UTM zone 32 North projection using the WGS-84 datum.

2.3 Image processing methods

Principal Component Analysis (PCA) (known as eigenvector-eigenvalue decomposition) is a statistical technique which is used to transform multidimensional data by reducing the variance and projecting the data along uncorrelated axes. It transforms a set of correlated input bands into uncorrelated spectral bands as principal components. The PCA is widely employed on multispectral data purposely to extract unique spectral responses such as hydrothermal alteration for geologic mapping and mineral exploration purposes (Gupta et al., 2013). In the present study, the feature-oriented principal component selection (FPCS) (Crosta and Moore, 1989), was employed in order to map specific hydrothermal alteration minerals of interest. Thus, the bands in which the targeted minerals, which are indicators of hydrothermal alteration related to geothermal systems were selected for the analysis. This was performed separately for iron oxide/hydroxide minerals (hematite, limonite, and goethite) that have diagnostic absorptions within the VNIR region, and for hydroxyl (OH) bearing minerals (clays, carbonates and sulfates) that contain absorption features in the SWIR portion.

The whole concept behind FPCS is that, by reducing the number of input bands for PCA in such a way as to ensure that certain minerals (or materials) will not be mapped while increasing the likelihood that other interesting targets will be unambiguously mapped into only one of the PC images (Loughlin, 1991).

A feature oriented guided PCA involves selection of bands in which specifically targeted minerals (or materials) of interest are theoretically known to have diagnostic reflectance and or absorption characteristics, while including a band in which such targets do not manifest, thus, facilitating the manifestation of the targets in the main input bands. The results can then be interpreted by identifying the Eigenvector matrix to observe the weighing. The Eigenvectors could be positive or negative which indicates reflection or absorption respectively, however, if the loadings are positive in the reflective band of a mineral the image tone is shown by bright pixels, and if they are negative, the image tone is shown by bright pixels for the enhanced target mineral (Gupta et al., 2013).

3. RESULTS AND DISCUSSION

ASTER subset scene (1515 × 1515 pixels) covering the zones of Wikki and Mawulgo thermal springs in Yankari Park area was used for FPCS analysis. Band 1 of VNIR region and bands 5, 6 and 8 of SWIR subsystem were selected to accomplish FPCS analysis here. Band 1 was selected due to high reflectance features of clay alteration minerals in VNIR. Band 5 (2.14-2.18 μm) was selected to identify alunite absorption feature in 2.16μm; band 6 (2.18-2.22 μm) was selected to detect Kaolinite (2.20 μm) and band 8 (2.29-2.36 μm) for calcites (2.35 μm) (Pour and Hashim, 2011a; Rowan et al., 2003). Band 2 (0.63-0.69 μm), band 3 (0.78-0.86 μm) and band 4 (1.6-1.7 μm) of ASTER were not selected here to avoid the effects of high abundance soil materials in Savannah environments.

Band 4 represents the spectral region where all alteration minerals of hydroxyl-bearing (OH) manifest strong reflection. Bands 2 and 3 show the manifestation of both iron oxides and vegetation due to strong reflections in 0.63 to 0.86 μm region, respectively. The statistical results derived from FPCS transformation to selected bands of ASTER are shown in Table 1.

Input Bands	Band 1	Band 5	Band 6	Band 8	
Eigenvector Matrix					Variance (%)
PC 1	0.173479	0.513621	0.538524	0.645051	87.5
PC 2	-0.899214	-0.056769	-0.145648	0.408631	9.6
PC 3	-0.401646	0.349319	0.558380	**-0.636292**	2.5
PC 4	-0.000195	**-0.781631**	**0.613995**	0.109829	0.4

Table 1. Covariance eigenvector values of the FPCS for the selected bands (1, 5, 6, and 8 of ASTER) for Yankari selected subset scene.

As shown by the eigenvalues, the resulting PC1 eigenvector loadings and eigenvalues show that that PC1 contains 87.5% of the total data variance (Table 1). Overall scene brightness albedo and the topographic effect are responsible for the strong correlation between multispectral image bands (Loughlin, 1991). From the results in Table 1, it is observed that hydroxyl-bearing minerals will best be mapped in PC3 and PC4 because of the large negative eigenvector loadings at PC3 band 8 (-0.63) and large negative and positive loadings at PC4 bands 5 (-0.78) and 6 (0.61), which appear as opposite signs (Table 1). This means areas of possible carbonates alteration will appear as dark pixels in PC3 due to their strong absorption in bands 8, while sulfates and clays may appear as dark and bright pixels in PC4 because of the higher opposite signs in bands 5 and 6 in which these alteration minerals are known to have diagnostic absorption features in these bands.

The results of PC3 and PC4 are shown in Figures 2 and 3. This identified alteration zones served as a guide for understanding areas to focus subsequent analysis and field validation particularly in relation to their proximity to the thermal springs. The above results are observed to conform well to exposed alteration areas identified in the field especially around the Mawulgo thermal spring, which is less vegetated. The results also corroborate well especially with exposed alteration areas designated; W1, W2, M1 and M2 as can be seen in both PC3 and PC4 image maps (Figs. 2 and 3).

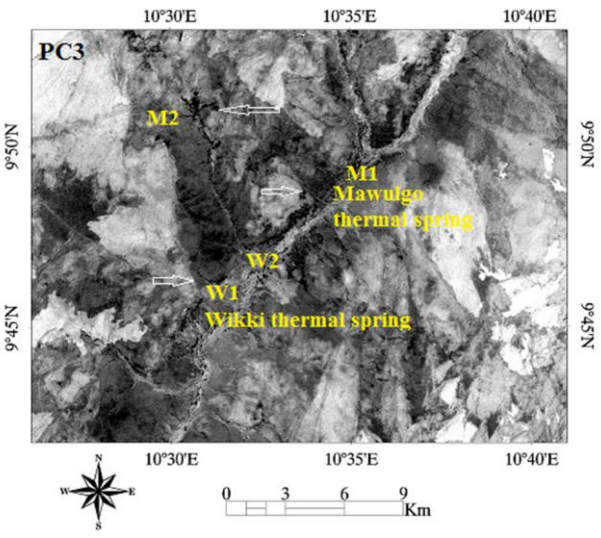

Figure 2. PC3 showing dark pixels as possible alteration zones due to hydroxyl-bearing minerals.

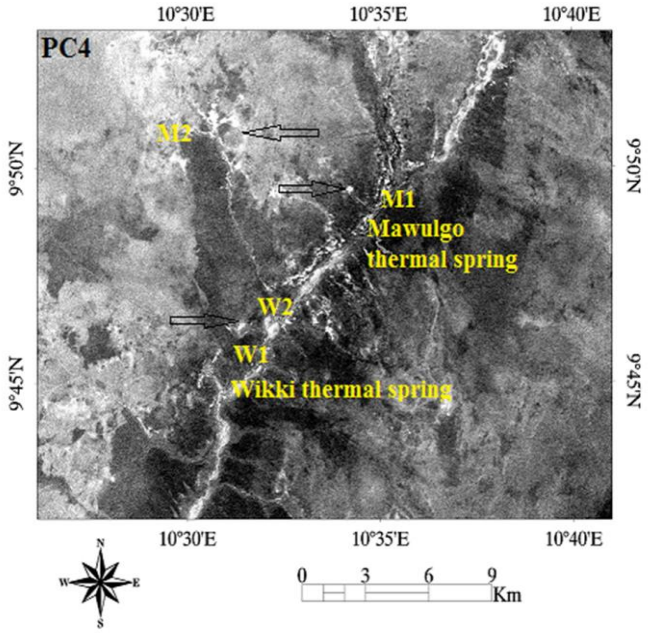

Figure 3. PC4 showing bright pixels as possible alteration zones due to hydroxyl-bearing minerals.

In this study, another FPCS was implemented to identify iron oxide alteration zones associated with geothermal systems using bands 1, 2 and 3 of the VNIR subsystem and band 4 of the SWIR subsystem of ASTER. Iron oxide/hydroxide minerals such as hematite, jarosite and limonite tend to have low reflectance in visible and higher reflectance in near infrared, coinciding with bands 1, 2 and 4 of ASTER data.

By observing the result of FPCS in Table 2, PC1 contains 80.32% of the total variance among the input bands, which implies that overall brightness and albedo is effectively mapped in PC1 as such may not contain spectra relevant for this analysis. The remaining PCs, however, shows a decreasing variance resulting from the PC 1, 2, 3 and 4. The PC2 appears to be appropriate to map iron oxide rich areas because of the large magnitude eigenvalue at PC2 band 2 (0.64) and moderate value at band 1 (0.40), which manifest possible areas of iron oxides as bright pixels in the PC2 image map (Fig. 4). It accounts for about 13% of the variance (Table 2). The negated low eigenvector value of PC2 in band 3 (-0.64) implies vegetated areas may appear as dark pixels because of vegetation manifest in the near infrared coincides with band 3 of ASTER. Consequently, along the Gaji river which is covered with vegetation appears as dark pixels (Fig. 4).

Generally, the results of the PCA effectively mapped and identified especially argillic alteration areas. However, there is some confusion in the iron oxide mapping in that area identified in the field as limonitic also appear as vegetated as observed in Figure 4. This may be attributable to the fact that most of the areas are covered by sparse vegetation and the alterations were territorially small not to be detected by the ASTER data, this was evident in the field especially around Wikki thermal spring.

Input Bands	Band 1	Band 2	Band 3	Band 4	
Eigenvector matrix					Variance (%)
PC 1	0.232547	0.425563	0.630823	0.605707	80.32
PC 2	**0.406700**	**0.640638**	-0.647698	**0.068307**	13.09
PC 3	-0.461241	-0.207888	-0.415524	0.755896	5.29
PC 4	0.753508	-0.604370	-0.099447	0.238902	1.29

Table 2. Covariance eigenvector values of the FPCS for the selected bands (1, 2, 3, and 4 of ASTER) for Yankari selected subset scene.

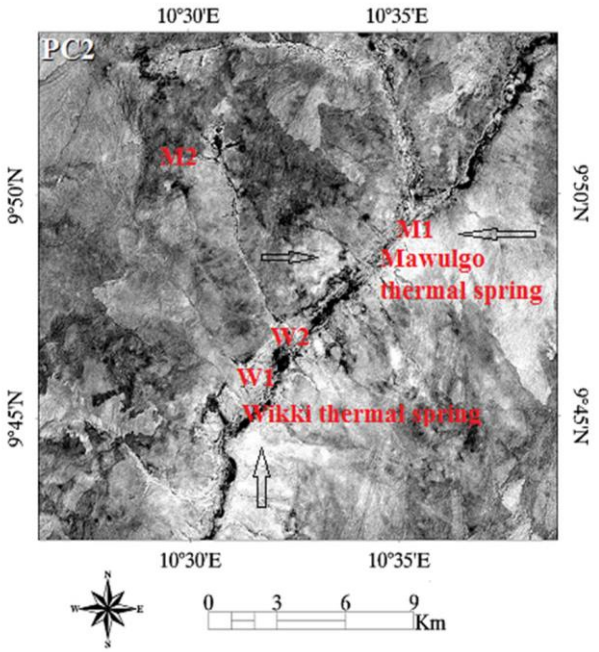

Figure 4. PC2 showing bright pixels as possible alteration zones due to iron oxide/hydroxide minerals.

It was observed that the alteration areas significantly conform to the identified areas during field work especially around Mawulgo thermal spring, where clay alterations were observed and the M designated samples are obtained. These are shown especially in PC3 dark pixels and PC4 dark and bright pixels for hydroxyl-bearing minerals in Figures 2 and 3, however, pixels appear unconformable when mapping iron oxides.

The result of the laboratory ASD and XRD analysis of rock samples acquired from alteration zones in the field were used to verify the image processing analysis. The results of representative collected rock samples from alteration zone analyzed in the laboratory conditions using XRD analysis are show the presence of kaolinite, illite, alunite, calcite, limonite, hematite, quartz and dickite as dominated alteration minerals in the collected rock samples.

During field survey was observed that the alteration types were predominantly limonitic around the Wikki thermal spring indicated by brownish to reddish iron oxides to hydroxide rock outcrops and argillic alterations indicated by bleached to gray-whitish rocks around areas of the Mawulgo thermal spring (see Fig. 5 a-d).

Figure 5. Field photographs of hydrothermal alteration mineral zones associated with the geothermal systems; (a) Exposed clay (argillic) alteration zone around Mawulgo thermal spring;(b) Carbonate alteration at Wikki thermal springs; (c) Exposed argillic altered rocks around Mawulgo thermal spring; (d) Vegetated areas of altered rocks around Wikki thermal spring.

4. CONCLUSIONS

In this study, we investigated the applicability of mapping hydrothermal alteration minerals associated with subtle geothermal systems using ASTER dataset as a proxy for identifying prospective sites of fossilized and concealed geothermal systems in the Yankari Park, northeastern Nigeria. Application of FPCS analysis to bands 5, 6 and 8 and bands 1, 2, 3 and 4 datasets of ASTER was used for mapping clay and iron oxide/hydroxide minerals in the zones of Wikki and Mawulgo thermal springs in Yankari Park area at the regional scale. The result of the laboratory, including ASD and XRD analysis of rock samples acquired from alteration zones in the field shows the presence of kaolinite, illite, alunite, calcite, limonite, hematite, quartz and dickite as dominated alteration minerals in the study zones. Therefore, the advanced argillic alteration was recorded for the Wikki and Mawulgo thermal springsin Yankari Park based on alteration mineral assemblages detected by image processing and fieldwork.

ACKNOWLEDGEMENTS

This study was conducted as a part of Tier 1 (vote no: Q.J130000.2527.13H13), research university grant category. We are thankful to the Universiti Teknologi Malaysia for providing the facilities for this investigation.

REFERENCES

Abrams, M. (2000). The Advanced Spaceborne Thermal Emission and Reflection Radiometer (ASTER): data products for the high spatial resolution imager on NASA's Terra platform. *international Journal of Remote sensing*. 21(5), 847-859.

Ajakaiye, D., Olatinwo, M. and Scheidegger, A. (1988). Another possible earthquake near Gombe in Nigeria on the 18-19 June 1985. *Bulletin of the Seismological Society of America*. 78(2), 1006-1010.

Calvin, W. M., Littlefield, E. F. and Kratt, C. (2015). Remote sensing of geothermal-related minerals for resource exploration in Nevada. *Geothermics*. 53, 517-526.

Calvin, W. M. and Pace, E. L. (2016). Mapping alteration in geothermal drill core using a field portable spectroradiometer. *Geothermics*. 61, 12-23.

Crosta, A. P. and Moore, J. M. (1989). Geological mapping using landsat thematic mapper imagery in Almeria province, south-east Spain. *International Journal of Remote Sensing*. 10(3), 505-514.

Gupta, R. P., Tiwari, R. K., Saini, V. and Srivastava, N. (2013). A simplified approach for interpreting principal component images.

Loughlin, W. (1991). Principal component analysis for alteration mapping. *Photogrammetric Engineering and Remote Sensing*. 57(9), 1163-1169.

Norton, D. L. (1984). Theory of hydrothermal systems. *Annual Review of Earth and Planetary Sciences*. 12, 155.

Pour, A. B. and Hashim, M. (2014). ASTER, ALI and Hyperion sensors data for lithological mapping and ore minerals exploration. *SpringerPlus*. 3(1), 1.

Pour, B.A., Hashim, M., 2015. Integrating PALSAR and ASTER data for mineral deposits exploration in tropical environments: a case study from Central Belt, Peninsular Malaysia. International Journal of Image and Data Fusion, 6(2), 170-188.

Pournamdary, M., Hashim, M., Pour, B.A., 2014a. Spectral transformation of ASTER and Landsat TM bands for lithological mapping of Soghan ophiolite complex, south Iran. Advances in Space Research 54 (4), 694-709.

Pournamdary, M., Hashim, M., Pour, B.A., 2014a. Application of ASTER and Landsat TM data for geological mapping of Esfandagheh ophiolite complex, southern Iran. Resource Geology 64 (3), 233-246.

U.S. Geological EROS, http://glovis.usgs.gov/; https://lpdaac.usgs.gov/dataset_discovery/aster/aster_products_table/ast_l1t.

Yamaguchi, Y. and Naito, C. (2003). Spectral indices for lithologic discrimination and mapping by using the ASTER SWIR bands. *International Journal of Remote Sensing*. 24(22), 4311-4323.